“© 2017 IEEE. Personal use of this material is permitted. Permission from IEEE must be obtained for all other uses, in any current or future media, including reprinting/republishing this material for advertising or promotional purposes, creating new collective works, for resale or redistribution to servers or lists, or reuse of any copyrighted component of this work in other works.”

Electrically Small Metamaterial-Inspired Antennas with Active Near Field Resonant Parasitic Elements: From Theory to Practice

Ming-Chun Tang[1] and Richard W. Ziolkowski[2,3] *
[1] College of Communication Engineering, Chongqing University, Chongqing, 400044, China, tangmingchun@cqu.edu.cn
[2] University of Technology Sydney, Global Big Data Technologies Centre, Ultimo NSW 2000, Australia
[3] Department of Electrical and Computer Engineering, University of Arizona, Tucson, AZ, USA,ziolkowski@ece.arizona.edu

***Abstract*—By augmenting several classes of metamaterial-inspired near-field resonant parasitic (NFRP) electrically small antennas (ESAs) with active (non-Foster) circuits, we have achieved performance characteristics surpassing their fundamental passive bounds. The designs not only have high radiation efficiencies, but they also exhibit large frequency bandwidths, large beam widths, large front-to-back ratios, and high directivities. Furthermore, the various initially theoretical and simulated designs have led to practical realizations. These active NFRP ESAs will be reviewed and recently reported designs will be introduced and discussed.**

***Index Terms*—Bandwidth, directivity, electrically small antennas, front-to-back ratio, Huygens source, parasitic elements**

I. Introduction

With the enormous economic impact of wireless systems and the fervor associated with the anticipation of potential IoT (internet of things) and future 5G systems, electrically small antennas (ESAs) have remained a topic of intense research interest in recent years because of their utility for a wide variety of wireless applications. However, because of their compact size, ESAs generally are not efficient radiators and have narrow bandwidths and low directivities. We review our contemporary successes to overcome the conflicting performance characteristics of ESAs, including their efficiencies, bandwidths, beam widths, directivities, and front-to-back ratios (FTBRs), by using a variety of meta-structures augmented with non-Foster elements.

II. Original Theoretical Concept

The basic idea of coupling an electrically small metamaterial-inspired near-field resonant parasitic (NFRP) element to a compact driven element to achieve an efficient ESA matched to a source with no matching network was introduced in [1]. These meta-structure-based ESAs have been verified experimentally and many others have since been developed and tested that achieve not only high efficiencies, but also multi-functionality by incorporating by design, several passive NFRP elements into the antenna system [2].

Non-Foster-augmented NFRP ESAs were first considered for enhancing their impedance bandwidth [3]. This was accomplished by designing a passive NFRP antenna whose resonance frequency was tunable simply by changing the value of an inductor or capacitor within its NFRP meta-structure and whose bandwidth came as close as possible to the Chu limit [4]. The specific values of those lumped elements which maintained the resonance frequency were first determined. It was found that a wide frequency-agile impedance bandwidth was obtained. Then a non-Foster circuit element was designed that instantaneously recovered those values as closely as possible. Replacing the fixed-value lumped component with its non-Foster counterpart, a wide impedance bandwidth ESA was achieved. This active NFRP element scheme is represented by the internal matching circuit concept illustrated in Fig. 1. It replaces the traditional approach in which an external non-Foster matching network is employed [5]-[7]. Because it theoretically only modifies the reactance behavior of the input impedance, rather than both its resistance and reactance, it removes many of the drawbacks associated with the traditional external active-circuit matching approach.

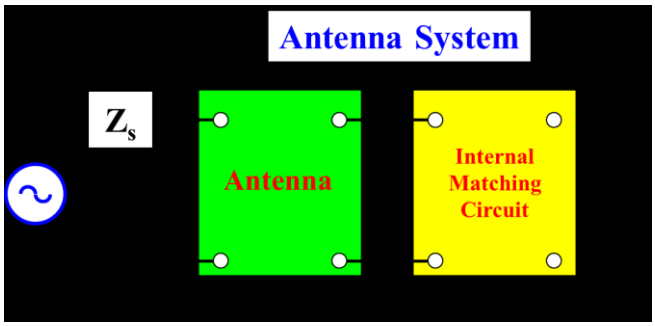

Fig. 1. The electrically small, NIC-augmented, near-field resonant parasitic (NFRP) antenna paradigm. The NIC circuit, which provides the required non-Foster inductance or capacitance behavior to maintain the resonance over a broad frequency bandwidth, is internal to the NFRP element and, hence, embedded within the antenna rather being external to it.

The canopy antenna design shown in Fig. 2, successfully demonstrated the advantage of the non-Foster-augmented NFRP antenna approach. The results were rather startling,

even theoretically. It was very electrically small with ka = 0.047, a being the radius of the smallest sphere enclosing the antenna and $k = 2\pi/\lambda$, λ being the free-space wavelength at its passive resonance frequency, 300 MHz, and it exhibited greater than a 10% -10-dB fractional impedance bandwidth.

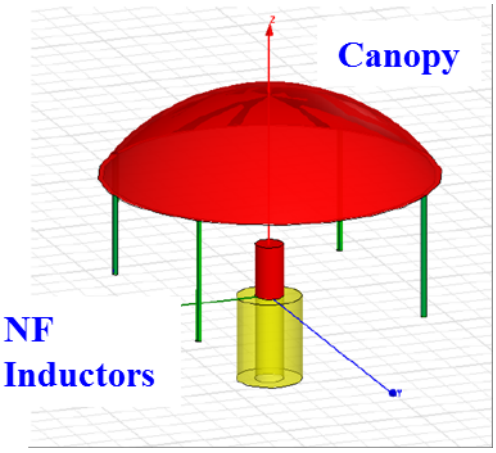

Fig. 2. Four-leg canopy antenna. Driven monopole, coax-fed through a ground plane, is covered with a copper canopy supported by four non-Foster inductor loaded legs. [1]

III. Non-Foster Realization

To physically demonstrate that one could indeed conquer the fundamental passive bound associated with the impedance bandwidth, non-Foster elements were introduced into the near-field resonant parasitic elements of two classes of metamaterial-inspired designs: the Egyptian axe dipole (EAD) and protractor antennas [8]-[11]. For example, the EAD antenna is shown in Fig. 3a. It is tunable by varying the inductor value incorporated into the EAD NFRP element. Its wide-bandwidth frequency agile response around 300 MHz is shown in Fig. 3b. The active non-Foster element of the EAD version was realized with a NIC-based inductor element, an L-NIC. A comparison of its non-Foster behavior with the desired one obtained from the results in Fig. 3b is shown in Fig. 3c.

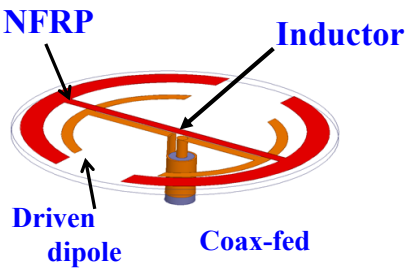

3(a)

The measurement of the impedance behavior of the prototype version of the L-NIC-augmented EAD antenna is shown in Fig. 3d. A comparison of the measured and predicted $|S_{11}|$ values as a function of the source frequency are shown in Fig. 3e. The realized impedance bandwidth was 5.77 times larger than the passive directivity over quality factor, D/Q, upper bound. Similar impedance bandwidth enhancements have been reported for related implementations [12], [13].

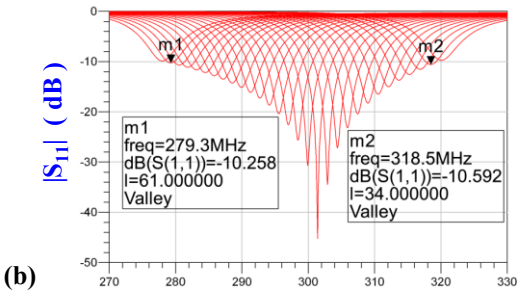

(b)

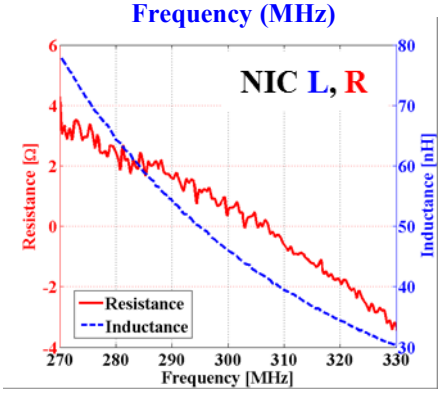

(c)

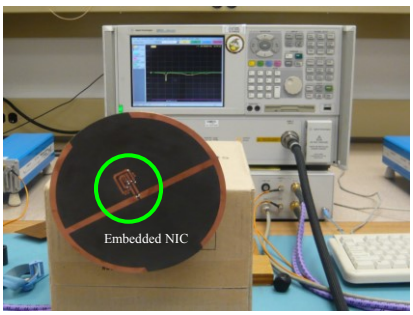

(d)

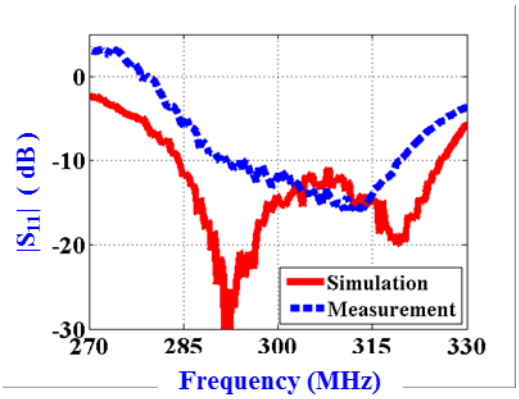

(e)

Fig.3. L-NIC augmented EAD ESA. (a) Isotropic view, (b) frequency agile behavior, (c) comparison of the ideal and L- NIC inductance values, (d) antenna under test, and (e) a comparison of predicted and measured $|S_{11}|$ values. [11]

IV. NFRP ESA WITH NO TRADE-OFFS

By introducing more NFRP elements into a metamaterial-inspired electrically small antenna system, one obtains more degrees of freedom which can be used to further enhance the characteristics of an ESA. For instance, beam width enhancements were achieved with a non-Foster augmented design [14]. By augmenting a high FTBR passive design that employed two NFRP elements [15] with both C-NIC and L-NIC non-Foster elements, a non-Foster-augmented ESA which has high efficiency, large impedance bandwidth, wide beam width, large front-to-back ratio, and high directivity (a Huygens source behavior), i.e., it has none of the usual trade-offs associated with ESAs, has been demonstrated [16]. This concept is illustrated in Fig. 4.

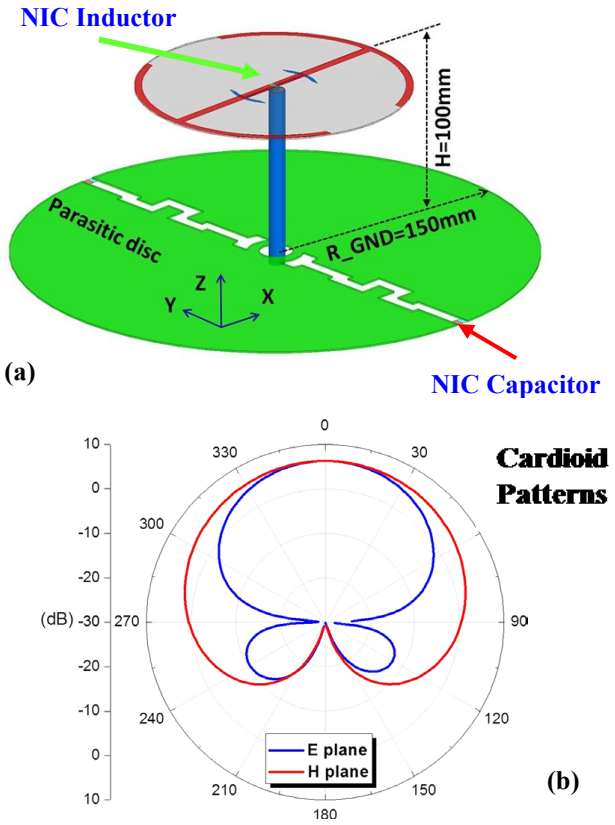

Fig. 4. Electrically small antenna with non-Foster augmented NFRP elements to achieve high radiation efficiency, large bandwidth, large FTBR and high directivity. (a) Basic configuration, and (b) the E- and H-plane directivity patterns at 300 MHz. [16]

The second NFRP element, the meanderline slot-based conductive disk was designed and tuned specifically for directivity enhancement of the EAD ESA. The EAD NFRP element was again augmented with a non-Foster L-NIC to enhance its impedance bandwidth. A meanderline-slotted metallic NFRP disk was added as shown in Fig. 4a to achieve the desired high directivity along with a large FTBR. It has two C-NIC elements incorporated into it at the outside ends of the slots. These increase the directivity bandwidth. The overall size of this particular design [16] was ka = 0.94. It achieved a directivity over quality factor more than 10 times the fundamental bound: $D/Q > 10 \times (D/Q)_{\text{passive ub}}$. As shown in Fig. 4b, its far-field has a cardioid directivity pattern. In particular, with a center frequency at 300 MHz, it simultaneously achieved high radiation efficiencies (> 81.63%), high directivities (> 6.25 dB), and large front-to-back-ratios (> 26.71 dB) over a 10.0% fractional bandwidth.

V. NON-FOSTER AUGMENTED HUYGENS SOURCE

The ESA shown in Fig. 4 was not low profile, i.e., its height was ~ λ_{res} / 10. Recall that Huygens equivalence principle, as demonstrated in [17], provides yet another means to achieve higher directivity with ESA systems. Consider an electric dipole source located in a specified plane. Then superimpose a magnetic dipole source to lie in the same plane and orient it to be orthogonal to the electric dipole. If their radiated field amplitudes are the same and if their phase centers are collocated, their combined result will be a Huygens source that radiates primarily into one of the half-spaces defined by the plane in which both sources are located and in a direction broadside to it. With a π phase shift in the excitation of either dipole source, this Huygens combination will radiate primarily in the opposite direction, i.e., into the other hemisphere. Thus, the key design issues are the dipole amplitudes, their phase centers, and their orientations.

A extremely low-profile (height ~ λ / 80), broadside radiating Huygens source ESA has been obtained by combining a driven, coax-fed printed dipole with an EAD NFRP element and two capacitively loaded loop (CLL) NFRP elements [18]. Because of the fine tuning needed to properly overlap the resonances of all of the NFRP elements, as well as to obtain similar radiated field amplitudes and collocated phase centers, its bandwidth was also very narrow. This drawback has been overcome with the slightly larger, but still low profile (height ~ λ / 20) non-Foster augmented NFRP ESA shown in Fig. 5 [19].

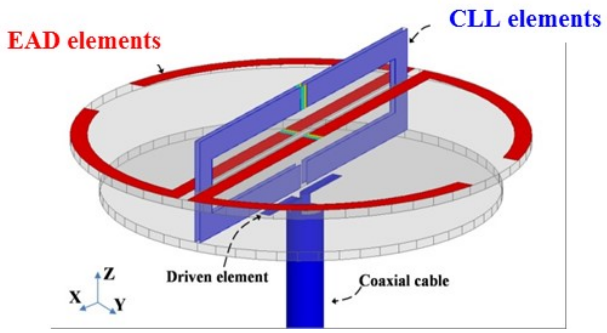

Fig. 5. Broad bandwidth Huygens source NFRP antenna augmented with four C-NICs, one C-NIC embedded in each of its four NFRP elements. [19]

This design [20] features a driven coax-fed printed dipole antenna combined with two CLL and two EAD meta-structures. Each of these NFRP elements is augmented with C-

NICs. When the ideal non-Foster components were introduced, the simulated impedance bandwidth witnesses approximately a 17-fold enhancement over the passive case. Within this -10dB bandwidth, its maximum realized gain, radiation efficiency, and front-to-back ratio (FTBR) are, respectively, 4.00 dB, 88%, and 26.95 dB. The $|S_{11}|$ values as a function of the source frequency and its 3D and 2D directivity patterns are shown in Fig. 6. When the anticipated actual negative impedance convertor (NIC) circuits are incorporated, the impedance bandwidth still sustains more than a 10-fold enhancement. The peak realized gain, radiation efficiency, and FTBR values of this realistic design are, respectively, 3.74 dB, 80%, and 28.01 dB, which are very comparable to the ideal values. While this non-Foster augmented Huygens source ESA has not yet been fabricated and tested, a related passive version has been measured [20]. The results have confirmed the Huygens source behavior of the design.

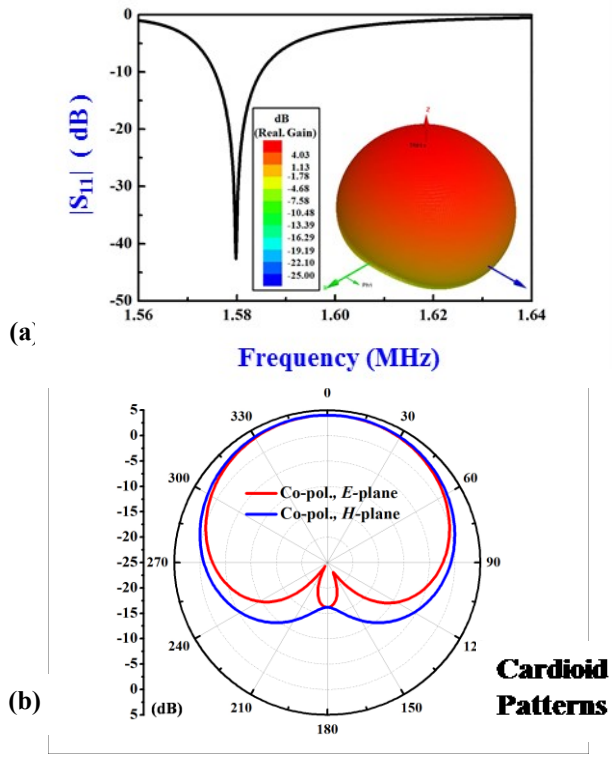

Fig. 6. The Huygens source ESA performance characteristics. (a) $|S_{11}|$ values as a function of the frequency and the 3-D realized gain pattern at f_{res}, and (b) the 2-D realized gain patterns in the E- and H- planes at f_{res} = 1.580 GHz. [19]

VI. CONCLUSION

It has been demonstrated that several combinations of meta-structure NFRP elements augmented with non-Foster elements can yield ESAs with performance characteristics surpassing their known passive bounds. Several of these designs have been fabricated and successfully tested. The concepts and realized designs will be discusses in our presentation. Additional practical issues, such as stability of the non-Foster circuits and non-Foster augmented ESAs, will also be discussed.

References

[1] A. Erentok and R. W. Ziolkowski, "Metamaterial-inspired efficient electrically-small antennas," IEEE Trans. Antennas Propag., vol. 56, no. 3, pp. 691-707, March 2008.

[2] R. W. Ziolkowski, P. Jin, and C.-C. Lin, "Metamaterial-inspired engineering of antennas," Proc. IEEE, vol. 99, no.10, pp.1720-1731, Oct. 2011.

[3] P. Jin and R. W. Ziolkowski, "Broadband, efficient, electrically small metamaterial-inspired antennas facilitated by active near-field resonant parasitic elements," IEEE Trans. Antennas Propag., vol. 58, pp. 318-327, Feb. 2010.

[4] L. J. Chu, "Physical limitations of omni-directional antennas," J. Appl. Phys., pp. 1163–1175, Dec. 1948.

[5] S. E. Sussman-Fort, "Matching network design using non-Foster impedances," Int. J. RF Microw. Comp. Eng., vol. 16, no. 2, pp. 135-142, Mar. 2006.

[6] J. T. Aberle and R. Lopesinger-Romak, *Antenna with Non-Foster Matching Networks*, San Rafael, CA: Morgan & Claypool Publishers, 2007.

[7] S. E. Sussman-Fort and R. M. Rudish, "Non-Foster impedance matching of electrically-small antennas," IEEE Trans. Antennas Propag., vol. 57, no. 8, pp. 2230-2241, Aug. 2009.

[8] N. Zhu and R. W. Ziolkowski, "Active metamaterial-inspired broad bandwidth, efficient, electrically small antennas," IEEE Antennas Wireless Propag. Lett., vol. 10, pp. 1582-1585, 2011.

[9] N. Zhu and R. W. Ziolkowski, "Broad bandwidth, electrically small antenna augmented with an internal non-Foster element," IEEE Antennas Wireless Propag. Lett., vol. 11, pp. 1116-1120, 2012.

[10] N. Zhu and R. W. Ziolkowski, "Design and measurements of an electrically small, broad bandwidth, non-Foster circuit-augmented protractor antenna," Appl. Phys. Lett., vol. 101, 024107, Jul. 2012.

[11] N. Zhu and R. W. Ziolkowski, "Broad bandwidth, electrically small, non-Foster element-augmented antenna designs, analyses, and measurements," IEICE Transactions on Communications, vol. E96-B, no.10, pp. 2399-2409, Oct. 2013.

[12] H. Mirzaei and G. V. Eleftheriades, "A resonant printed monopole antenna with an embedded non-Foster matching network," IEEE Trans. Antennas Propag., vol 61, no. 11, pp. 5363-5371, Nov. 2013

[13] J. Church, J.-C. Chieh, L. Xu, J. D. Rockway and D. Arceo, "UHF electrically small box cage loop antenna with an embedded non-Foster load," Antennas Wirel. Propag. Lett., vol. 13, pp. 1329-1332, 2014.

[14] M.-C. Tang, N. Zhu and R. W. Ziolkowski, "Augmenting a modified Egyptian axe dipole antenna with non-Foster elements to enlarge its directivity bandwidth," IEEE Antennas Wireless Propag. Lett., vol. 12, pp. 421-424, 2013.

[15] M.-C. Tang, and R. W. Ziolkowski, "Efficient, high directivity, large front-to-back-ratio, electrically small, near-field-resonant-parasitic antenna," IEEE Access, vol. 1, no. 1, pp. 16 - 28, May 2013.

[16] R. W. Ziolkowski, M.-C. Tang and N. Zhu, "An efficient, broad bandwidth, high directivity, electrically small antenna," Microw. Opt. Technol. Lett., vol. 55, no. 6, pp. 1430-1434, June 2013.

[17] P. Jin, and R. W. Ziolkowski, "Metamaterial-inspired, electrically small Huygens sources," IEEE Antennas Wirel. Propag. Lett., vol. 9, pp. 501-505, 2010.

[18] R. W. Ziolkowski, "Low profile, broadside radiating, electrically small Huygens source antennas," IEEE Access, vol. 3, pp. 2644-2651, Dec. 2015.

[19] M.-C. Tang, T. Shi, and R. W. Ziolkowski, "Electrically small, broadside radiating Huygens source antenna augmented with internal non-Foster elements to increase its bandwidth," to appear in IEEE Antennas Wirel. Propag. Lett., 2016

[20] M.-C. Tang, H. Wang, and R. W. Ziolkowski, "Design and testing of simple, electrically small, low-profile, Huygens source antennas with broadside radiation performance," to appear in IEEE Trans. Antennas Propag., 2016.